

## Commission H (Waves in Plasmas) Activity Report

July 31, 2010

T. Okada, and Y. Omura

## Research Topics

## Akebono

The characteristics of wire antennas in space plasma are necessary to determine the absolute intensity and the phase of the electric field waves, because the observation data are given by voltage signals. One of the important characteristics of wire antennas is the antenna impedance. Determination of the impedance can be especially difficult since the impedance depends on the surrounding plasma environment, and the impedance is affected primarily by the plasma sheath created around the antenna. In Higashi et al. [2010], the dependences of the antenna impedance on the geomagnetic field and the plasma wake formed around the satellite body have been analyzed, according to the statistical analysis of measurement results of the antenna impedance for 15 years on Akebono satellite.

Kitamura et al. [2009] statistically studied meridional electron density distributions above  $45^\circ$  invariant latitude (ILAT) during geomagnetically quiet periods. Electron density data were obtained from plasma waves observed by the Akebono satellite from March 1989 to February 1991 (near solar maximum) in an altitude range of 274-10,500 km. Field-aligned electron density profiles were fitted by the sum of exponential and power law functions. The transition height, where the power law term equals the exponential term, is highest in the summer (at low solar zenith angle (SZA)) at  $\sim 4000$  km and lowest in the winter (at high SZA) at  $\sim 1800$  km in a region of  $ILAT \geq 70^\circ$  this is caused by the larger scale height in the summer ( $\sim 550$  km) than that in the winter ( $\sim 250$  km).

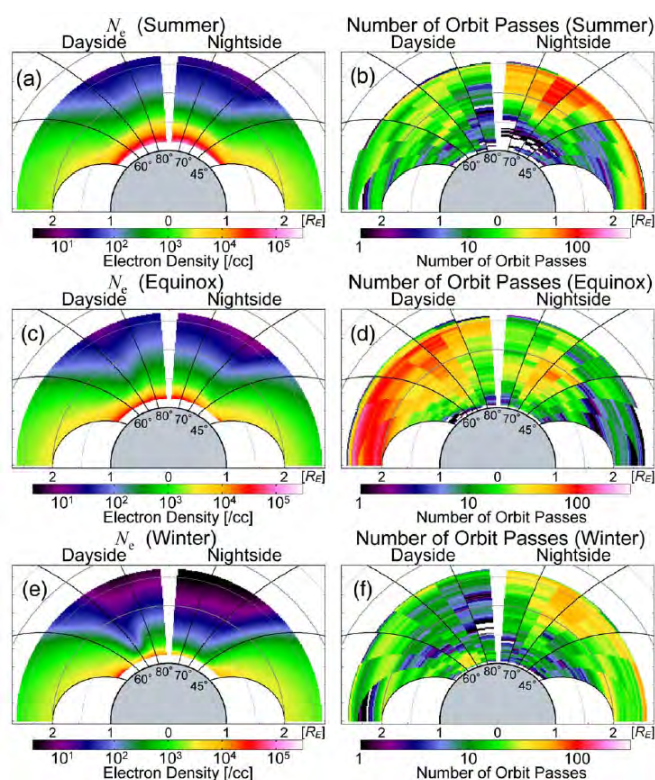


Figure 1. Electron number density distribution models in a region of  $ILAT > 45$  in an altitude range of 1000-10,500 km derived from the Akebono plasma wave data.

The largest seasonal variation and SZA dependence of the electron density are found at an altitude of  $\sim 2000$  km with a factor of  $\sim 50$  ( $\sim 10^4$  /cc in the summer,  $\sim 10^3$  /cc in the winter) in the trough, auroral, and polar cap regions. The seasonal variation and SZA dependence are smaller, about a factor of 5-10, above  $\sim 5000$  km.

Day-night asymmetries in each season (within a factor of 5) are smaller than the seasonal variation. The scale height is larger in the dayside than in the nightside in each season. These results indicate that photoionization processes in the ionosphere strongly control electron density distributions up to at least  $\sim 5000$  km in the trough, auroral, and polar cap regions. Figure 1 shows the electron number density distribution models in the polar region derived from the Akebono plasma wave data.

In order to understand temporal variations and spatial distributions of plasma density enhancements in the polar magnetosphere during geomagnetic storms, Kitamura et al. [2010] investigated nearly simultaneous observation data of storm time electron densities in the polar magnetosphere by the Akebono satellite and ion upflows in the polar ionosphere by the DMSP satellites. Akebono observations show that the electron densities were highest ( $>100$   $\text{cm}^{-3}$  at  $\sim 9000$  km altitude) from the main to early recovery phases of geomagnetic storms (Figure 2).

The regions of enhanced electron density were not localized but widely spread in the polar magnetosphere. Coordinated observations by the DMSP satellites detected ion upflows with large fluxes ( $\sim 10^{10}$  / $\text{cm}^2/\text{s}$ ) in and near the cusp, when the electron density enhancements were observed by the Akebono satellite. This result indicates that the storm time electron density enhancements are caused by cleft ion fountain mechanisms from the polar ionosphere. Very low-energy component ( $<13$  eV) of the cleft ion fountain drifted deep into the polar cap, and increased the plasma densities in a wide region of the polar cap and auroral zone. A large amount of the very low-energy plasma may flow out through the polar magnetosphere during the main phase of geomagnetic storms.

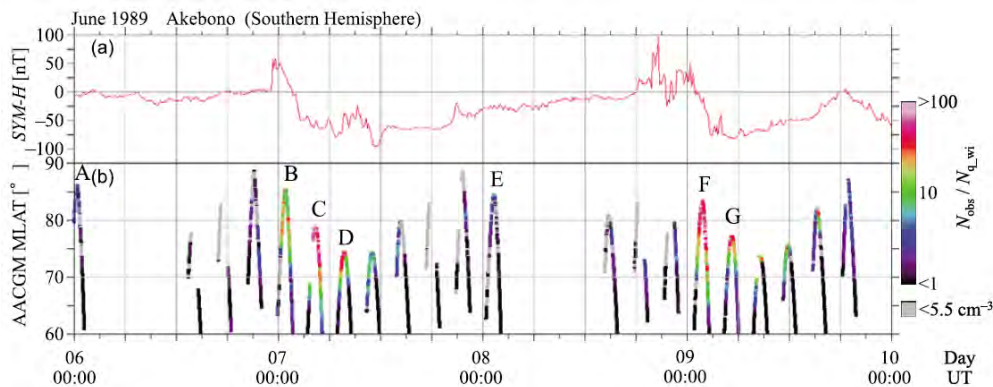


Figure 2. Storm time electron number density enhancements observed by the Akebono.

## References

- Higashi, R., T. Imachi, Y. Kasahara, S. Yagitani, and I. Nagano, "Statistical analysis of antenna impedance onboard akebono satellite," Proc. AP-RASC'10, Toyama, Japan, September 2010.
- Kitamura, N., Y. Nishimura, T. Ono, A. Kumamoto, A. Shinbori, M. Iizima, A. Matsuoka, and M. R. Hairston, Temporal variations and spatial extent of the electron density enhancements in the polar magnetosphere during geomagnetic storms, *J. Geophys. Res.*, 115, A00J02, doi:10.1029/2009JA014499, 2010.
- Kitamura, N., A. Shinbori, Y. Nishimura, T. Ono, M. Iizima, and A. Kumamoto, Seasonal variations of the electron density distribution in the polar region during geomagnetically quiet periods near solar maximum, *J. Geophys. Res.*, 114, A01206, doi:10.1029/2008JA013288, 2009.

## Geotail

Geotail spacecraft has observed many chorus emissions mainly in the Earth's dayside outer magnetosphere. Mori et al. [2010] have analyzed the waveform data of the chorus emissions and examined the relationship between the frequency sweep rates and the amplitudes of the chorus emissions. When a series of chorus emissions with almost the same propagation characteristics are observed in less than several seconds, interesting positive correlation between their frequency sweep rates and amplitudes are observed. The correlation seems to be changed with ambient plasma conditions as well as the Earth's magnetic field. On the basis of a statistical analysis of the chorus waveforms, they have discussed possible relationship among the frequency sweep rates and the amplitudes, as well as the amplitude variations (linear growth and subsequent nonlinear growth, saturation and decay) of the chorus emissions.

The Earth's bow shock is known to produce non-thermal electrons which are generally observed as a 'spike' in their flux profile. Oka et al. [2009] performed an analysis of electron and whistler wave properties for a quasi-perpendicular shock crossing that is supercritical, but subcritical to the so-called whistler critical Mach number above which whistler waves cannot propagate upstream (Figure 3). They have found that the amplitudes of whistler waves increased exponentially as a function of time prior to the shock encounter, while the suprathermal (>2 keV) electron flux similarly increased with time, although with differing e-folding time scales.

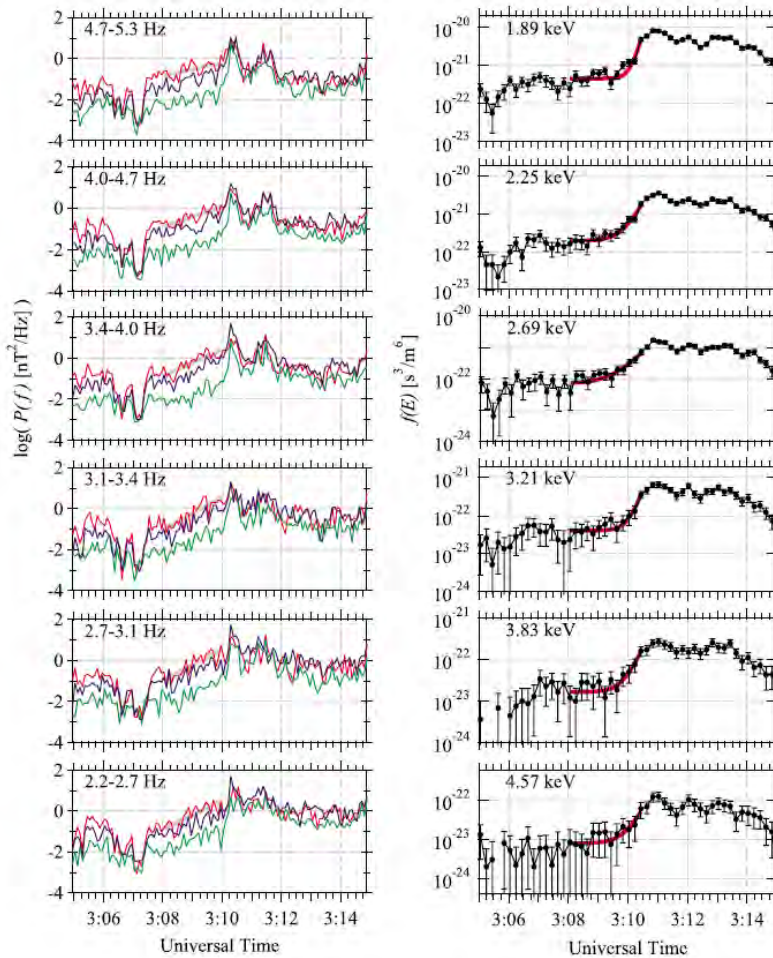


Figure 3. Whistler waves (Left panels) and electrons (Right panels) at quasi-perpendicular shock crossing

Comparison of the electron energy spectrum measured within the ramp with predictions from diffusive shock acceleration theory was poor, but the variation of pitch angle distribution showed scattering of non-thermal electrons in the upstream region. While not finding a specific mechanism to account for the electron diffusion, they suggest that the whistlers seen probably account for the differences observed between this 'gradual' event and the 'spike' events seen at shocks with no upstream whistlers.

Energetic ions are at times observed in the upstream region of the Earth's bow shock, and their origin is considered to be in the interaction with the shock front. While the energy of the solar wind ions is a few keV at most, the energy of the back streaming ions ranges from ~5 keV to several MeV. Seki et al. [2009] investigated back streaming energetic ions in the upstream of the Earth's bow shock observed by Geotail during two coronal mass ejection events (Figure 4). The observed local magnetic field rotated significantly during the events. Using the bow shock model and the observed magnetic field data, they found that the energetic ions appeared only when the upstream magnetic field was connected to the bow shock. The energetic ions showed two distinct distribution function characteristics, namely, the field-aligned beam (FAB) and the loss cone-shaped distribution. While the former is occasionally detected, the latter having higher energies (30 keV to several hundred keV, compared to <18 keV for FAB) has not been reported before. Using a bow shock model, they can also estimate the shock angle at the point on the shock surface that the upstream field line is connected to and find that the distribution function shape transits from the FAB to the loss cone-shaped distribution as the shock angle becomes larger (transition at  $\Theta_{Bn} = 70^\circ\text{-}80^\circ$ ). They discuss the possible mechanisms responsible for the production of the newly found member of the energetic upstream ion family.

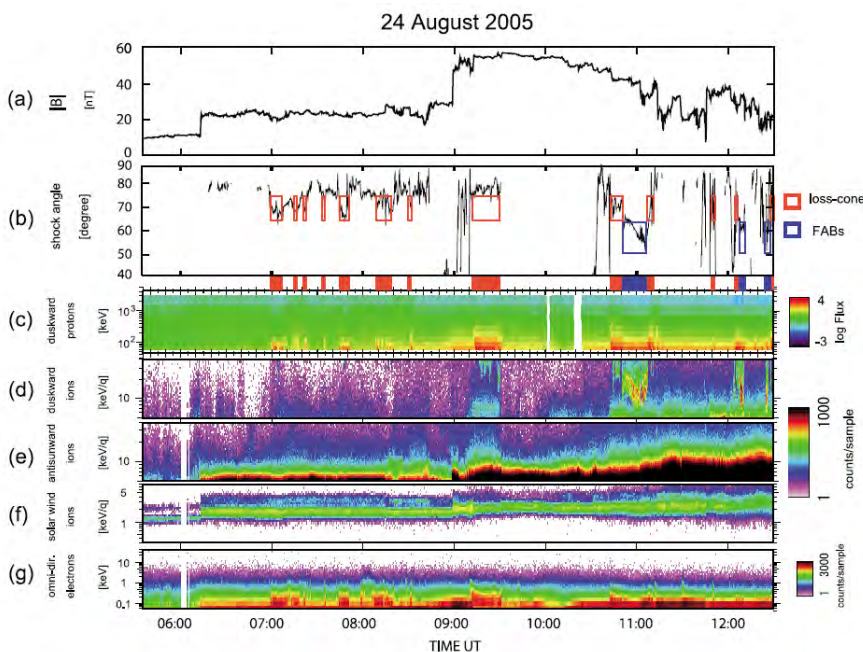


Figure 4. Overview of Geotail observations with indication of loss-cone-shaped back streaming energetic protons upstream of the Earth's bow shock

#### References:

- Mori, S., S. Yagitani, M. Hikishima, and H. Kojima, "Frequency and amplitude variation of chorus emissions observed by GEOTAIL," Proc. AP-RASC'10, Toyama, Japan, September 2010.
- Oka, M., T. Terasawa, M. Fujimoto, H. Matsui, Y. Kasaba, Y. Saito, H. Kojima, H. Matsumoto, T. Mukai, Non-thermal electrons at the Earth's bow shock: A 'Gradual' event, *Earth, Planets, Space*, 61, 603-606, 2009.

Seki, Y., M.N. Nishino, M. Fujimoto, Y. Miyashita, K. Keika, H. Hasegawa, K. Okabe, Y. Kasaba, T. Terasawa, T.I. Yamamoto, I. Shinohara, Y. Saito, and T. Mukai, Observations of loss-cone shaped backstreaming energetic protons upstream of the Earth's bow shock, *J. Geophys. Res.*, 114, A11106, doi:10.1029/2009JA014136, 2009.

### Antenna analysis

Imachi et al. [2010] have analyzed the method to estimate the characteristics of the wire antenna theoretically. In their analysis, the electric field is assumed to be a distribution of electrostatic potential, and the environment surrounding the wire antenna, including the structure of the wire and the receiver is written into an equivalent circuit. Using the analysis, they can estimate the characteristics of the wire antenna, such as the effective length, the impedance and the pickup factor, including the effect of the detailed structure of the wire, such as the wire insulator and the noise reduction shield.

### References:

Imachi, T., S. Yagitani, R. Higashi. and I. Nagano, "Characteristics of wire antenna for plasma wave observation at low frequencies," *Proc. AP-RASC'10*, Toyama, Japan, September 2010.

### Techniques of Data Analysis and Computer Experiments

As the total amount of data measured by scientific spacecraft is drastically increasing, it is necessary for researchers to develop new computation methods for efficient analysis of these enormous datasets. Kasahara et al. (2010) proposed a new algorithm for similar data retrieval. The aim of their study is to develop a technique to discover interesting and/or epoch-making datasets from enormous datasets. Many types of computational methods have already been devised and tested for achieving this. Some of these were developed based on learning algorithms such as neural network and pattern recognition. These algorithms work very powerfully to retrieve the required datasets from enormous databases if the characteristics of the required datasets are well known. However, it is also important for scientists in geophysics and space physics to discover new and unusual phenomena.

In order to solve this problem, Kasahara et al. (2010) constructed a database system on VLF/ELF waves obtained by the MCA onboard Akebono and introduced several kinds of key descriptors, such as wave intensity, time variation of wave spectrum, and ratio between electric and magnetic wave components, in order to describe the distinctive wave spectrum features. Finally they applied a proposed algorithm for

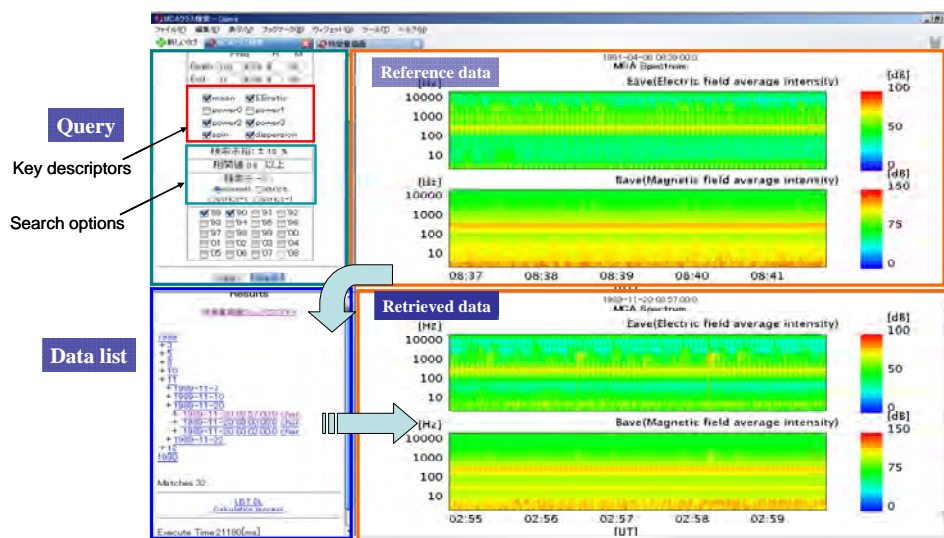


Figure 5: A snapshot of the event finding system (Kasahara et al., 2010).

similar data retrieval by storing these key descriptors in the database and evaluated the performance of the system. It was demonstrated that the developed algorithm works well for the purpose of similar data retrieval, and its computation time is also small enough for practical use. It is especially notable that the generality of the system is taken into account so that the proposed method is applicable not only to MCA data but also to other kinds of datasets.

**References:**

Y. Kasahara, A. Hirano and Y. Takata, Similar Data Retrieval from Enormous Datasets on ELF/VLF Wave Spectrum Observed by Akebono, *Data Science Journal*, 8, IGY66-IGY75, doi:10.2481/dsj.SS\_IGY-002, 2010.

**Computer simulation**

Kalaei et al. [2009] investigated a linear mode conversion process among UHR-mode, Z-mode and LO-mode waves by a computer simulation solving Maxwell’s equations and the motion of a cold electron fluid (Figure 6). The characteristics of the wave coupling process occurring in the cold magnetized plasma were examined in detail for the case of an inhomogeneity of plasma density lying perpendicular to the ambient magnetic field. The results show that efficient conversion processes take place under the specific condition of the wave normal angle of the incident UHR-mode waves in which the perpendicular component of the refractive index becomes zero at the site of mode conversion. They revealed that the range of this critical wave normal angle varies depending on both plasma frequency and frequency of incident UHR-mode waves. Their simulation results clarified that, by considering the steepness of the density gradient, efficient mode conversion could be expected even in the case of the mismatch of refractive indexes preventing the close coupling of plasma waves.

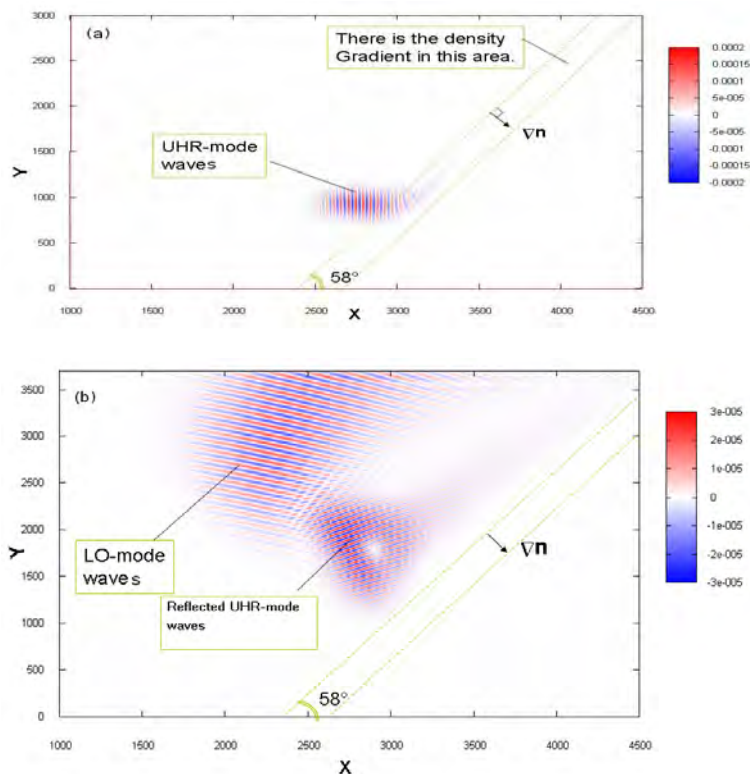


Figure 6. Spatial distributions of the Ex component of the electric field in the simulation system

at (a)  $t=52.5 \omega_c^{-1}$  and at (b)  $t=157 \omega_c^{-1}$ .

## References

Kalaei, M. J., T. Ono, Y. Katoh, M. Iizima, and Y. Nishimura, Simulation of mode conversion from UHR-mode wave to LO-mode wave in an inhomogeneous plasma with different wave normal angles, *Earth Planets Space*, 61, 1243-1254, 2009.

## KAGUYA (SELENE)

The Japanese lunar explorer “KAGUYA” was launched on September, 14, 2007 and the operation was successfully performed until KAGUYA was impacted to the south-east of near side of the moon on June 10, 2009. The Lunar Radar Sounder (LRS) is one of the scientific instruments onboard the KAGUYA main orbiter. The LRS consists of two orthogonal 30 m tip-to-tip antennas and three subsystems; the sounder observation (SDR), the natural plasma wave receiver (NPW), and the waveform capture (WFC). The SDR is designed to investigate the surface and subsurface structures of the moon using an HF radar technique, and the NPW and WFC are designed to measure natural plasma waves around the moon and in interplanetary space.

Because the moon is basically non-magnetized, the solar wind particles directly hit the lunar surface and a plasma cavity called the “lunar wake” is created behind the moon. Hashimoto et al. (2010) presented observations of electrostatic solitary waves (ESWs) near the Moon in the solar wind and in the lunar wake. They demonstrated that ESWs are categorized into three types depending on different regions of observations: ESWs generated by electrons reflected and accelerated by an electric field in the wake boundary (Type A), strong ESWs generated by bi-streaming electrons mirror-reflected over the magnetic anomaly (Type B), and ESWs generated by reflected electrons when the local magnetic field is connected to the lunar surface (Type C).

Nishino et al. (2010) studied effect of the solar wind (SW) proton entry deep into the near-Moon wake that was recently discovered by the KAGUYA spacecraft. Because previous lunar-wake models are based on electron dominance, no effect of SW proton entry has been taken into account. They showed that the type-II entry of SW protons forms proton-governed region (PGR) to drastically change the electromagnetic environment of the lunar wake. Broadband electrostatic noise found in the PGR is manifestation of electron two-stream instability, which is attributed to the counter-streaming electrons attracted from the ambient SW to maintain the quasi-neutrality. Acceleration of the absorbed electrons up to  $\sim 1$  keV means a superabundance of positive charges of  $10^{-5}\sim 10^{-7}\text{cm}^{-3}$  in the near-Moon wake, which should be immediately canceled out by the incoming high-speed electrons. They demonstrated that this is a general phenomenon in the lunar wake, because PGR does not necessarily require peculiar SW conditions for its formation.

The Lunar Radar Sounder (LRS) onboard the Kaguya (SELENE) spacecraft successfully obtained 2363-hours worth of radar sounder data and 6570-hours worth of natural plasma wave data in the nominal operation period from October 29, 2007 to September 10, 2008 and 2390-hours worth of natural plasma wave data in the extended operation period until June 10, 2009 [Ono et al. 2010]. Ono et al. [2009] found that there are distinct subsurface reflectors with a depth of several hundred meters below the surface of the nearside maria (Figure 7). The reflectors are inferred to be old regolith layers covered by basalt layers. Based on further analyses, Oshigami et al [2009] reported that the subsurface echoes are found only in 10% of the western nearside maria such as Mare Humorum, Mare Imbrium, and Oceanus Procellarum. Pommerol et al. [2010] also suggested that detectability of the subsurface echoes depend on abundance of TiO<sub>2</sub> and FeO in the surface material. Kobayashi et al. [2010] proposed the estimation method of the thickness of the surface regolith by the apparent difference of altitudes measured by laser altimeter (LALT) and LRS. It enables us to obtain regolith thickness with several m, which is much less than the range resolution of LRS, or 75m. LRS was operated not only for the radar sounder observation but also for the passive radio wave observation. Through the operation period from October 2007 to September 2008,

numerous events of auroral kilometric radiation (AKR), 39 events of type III solar radio bursts, and 7 events of Jovian hectometric (HOM) radiation were detected.

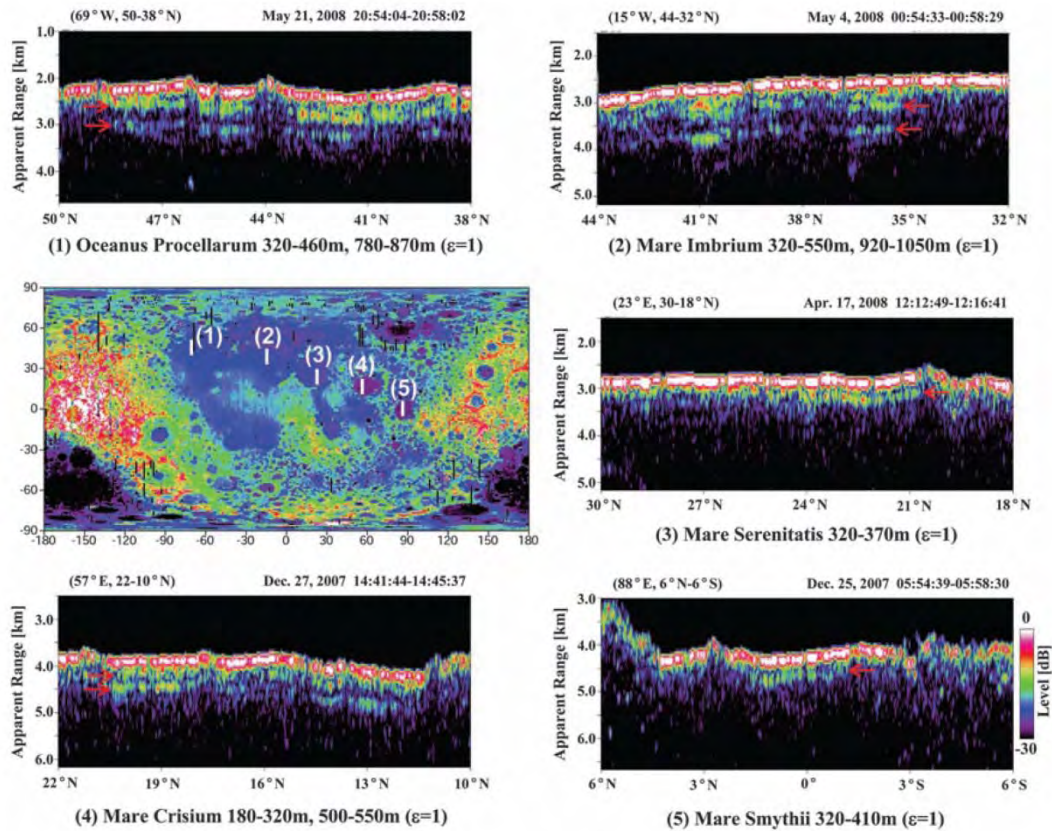


Figure 7. Subsurface reflectors found in the nearside maria of the moon

## References

- Hashimoto K. , M. Hashitani, Y. Kasahara, Y. Omura, M. N. Nishino, Y. Saito, S. Yokota, T. Ono, H. Tsunakawa, H. Shibuya, M. Matsushima, H. Shimizu, and F. Takahashi, Electrostatic solitary waves associated with magnetic anomalies and wake boundary of the Moon observed by KAGUYA, *Geophys. Res. Lett.*, (accepted for publication), 2010.
- Kobayashi, T., J. H. Kim, S. R. Lee, H. Araki, and T. Ono, Simultaneous Observation of Lunar Radar Sounder and Laser Altimeter of Kaguya for Lunar Regolith Layer Thickness Estimate, *IEEE LGRS*, 7, 3, 435-439, doi:10.1109/LGRS.2009.2038499, 2010.
- Ono, T., A. Kumamoto, H. Nakagawa, Y. Yamaguchi, S. Oshigami, A. Yamaji, T. Kobayashi, Y. Kasahara, and H. Oya, Lunar Radar Sounder Observations of Subsurface Layers under the Nearside Maria of the Moon, *Science*, 323, 5916, 909-912, doi:10.1126/science.1165988, 2009.
- Nishino N.M., M. Fujimoto, Y. Saito, S. Yokota, Y. Kasahara, Y. Omura, Y. Goto, K. Hashimoto, A. Kumamoto, T. Ono, H. Tsunakawa, M. Matsushima, F. Takahashi, H. Shibuya, H. Shimizu, and T. Terasawa, Effect of the solar wind proton entry into the deepest lunar wake, *Geophys. Res. Lett.*, 37, L12106, doi:10.1029/2010GL043948, 2010.
- Ono, T. ,A. Kumamoto, Y. Kasahara, Y. Yamaguchi, A. Yamaji, T. Kobayashi, S. Oshigami, H. Nakagawa, Y. Goto, K. Hashimoto, Y. Omura, T. Imachi, H. Matsumoto, H. Oya, The Lunar Radar Sounder (LRS) onboard the KAGUYA (SELENE) spacecraft, *Space Science Review*, (accepted for publication), 2010.
- Oshigami, S., Y. Yamaguchi, A. Yamaji, T. Ono, A. Kumamoto, T. Kobayashi, H. Nakagawa, Distribution of the subsurface reflectors of the western nearside maria observed from Kaguya with Lunar Radar

Sounder, *Geophys. Res. Lett.*, 36, L18202, doi:10.1029/2009GL039835, 2009.

Pommerol, A., W. Kofman, J. Audouard, C. Grima, P. Beck, J. Mouginot, A. Herique, A. Kumamoto, T. Kobayashi, T. Ono, Detectability of subsurface interfaces in lunar maria by the LRS/SELENE sounding radar: Influence of mineralogical composition, *Geophys. Res. Lett.*, 37, L03201, doi:10.1029/2009GL041681,2010.

## BepiColombo

The BepiColombo Mercury Magnetospheric Orbiter (MMO) spacecraft includes the plasma and radio wave observation system called Plasma Wave Investigation (PWI). Kasaba et al. [2010] reviewed the significance and objectives of plasma/radio wave observations in the Hermean magnetosphere, and describes the PWI sensors, receivers and their performance as well as the onboard data processing. Since the receivers for electric field, plasma waves, and radio waves are not installed in any of the preceding spacecraft to Mercury, the PWI will provide the first opportunity for conducting in-situ and remote-sensing observations of electric fields, plasma waves, and radio waves in the Hermean magnetosphere and exosphere. These observations are valuable in studying structure, dynamics, and energy exchange processes in the unique magnetosphere of Mercury. They are characterized by the key words of the non-MHD environment and the peculiar interaction between the relatively large planet without ionosphere and the solar wind with high dynamic pressure. The PWI consists of three sets of receivers (EWO, SORBET, and AM<sup>2</sup>P), connected to two sets of electric field sensors (MEFISTO and WPT) and two kinds of magnetic field sensors (LF-SC and DB-SC) (Figure 8). The PWI will observe both waveforms and frequency spectra in the frequency range from DC to 10 MHz for the electric field and from 0.3 Hz to 640 kHz for the magnetic field. From 2008, they will start the development of the engineering model, which is conceptually consistent with the flight model design.

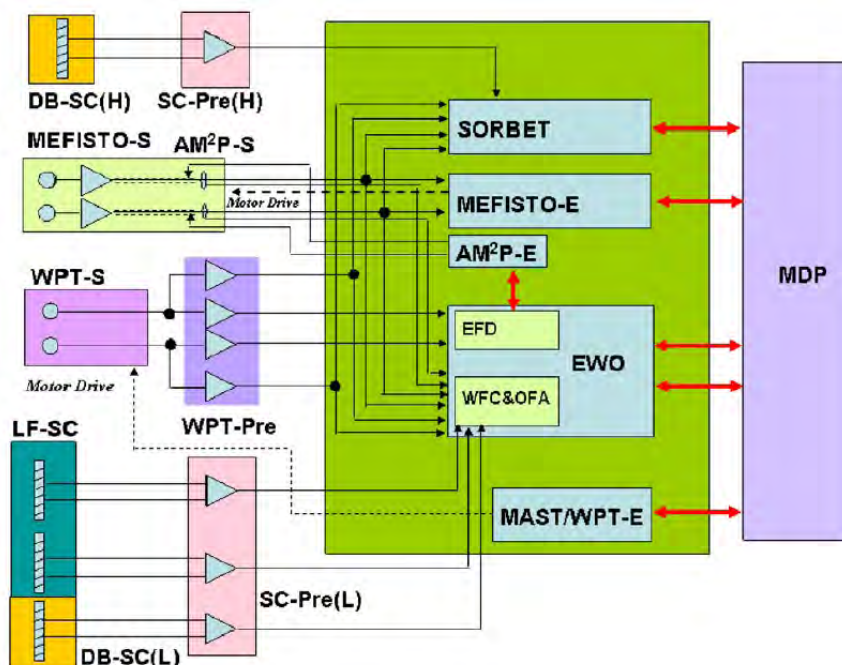


Figure 8. Block diagram of the PWI system onboard the BepiColombo/MMO

## References:

Kasaba, Y., J.-L. Bougeret, L.G. Blomberg, H. Kojima, S. Yagitani, M. Moncuquet, J.-G. Trotignon, G.

Chanteur, A. Kumamoto, Y. Kasahara, J. Lichtenberger, Y. Omura, K. Ishisaka, and H. Matsumoto, The Plasma Wave Investigation (PWI) onboard the BepiColombo / MMO: First measurement of electric fields, electromagnetic waves, and radio waves around Mercury, Planet. Space Sci., 58, 238-278, 2010.

## ULF Waves

Ikeda et al. (2010) examined nighttime Pi2 pulsations simultaneously observed by a Frequency Modulated Continuous Wave (FM-CW) HF radar and by a ground magnetometer, both located at a mid-latitude ( $L=2.05$ ) station belonging to the Magnetic Data Acquisition System (MAGDAS). They observed 83 Pi2 events in 43 days. The ground magnetic  $H$  component and the ionospheric Doppler velocity ( $V^*$ ) exhibited high coherence for 80% of the 83 events, and about half of the high-coherence events had the same dominant frequency in  $H$  and  $V^*$ . For such events,  $V^*$  led  $H$  by  $90^\circ$  in phase in the midnight sector of 2230–0300 LT (This  $90^\circ$  phase lag was not found for the five events observed near dusk or dawn.) The phase relation of  $H$  and  $V^*$  in the midnight sector may be explained in terms of the radial standing structure of compressional waves, i.e., cavity mode oscillation.

Obana et al. (2010a) cross-phase analyzed the data from a ground magnetometer array, and determined the equatorial mass density during three moderate geomagnetic storms. In each case the field line eigenfrequency increased significantly, suggesting the depletion of flux tubes and the earthward motion of the plasmapause. They then estimated the rate at which these flux tubes were refilled to prestorm levels; the result was 2–3 days for  $L=2.3$  flux tubes, 3 days at  $L=2.6$ , and  $>4$  days at  $L>3.3$ . The refilling progressed with a clear diurnal variation (linearly increasing plasma density in the daytime and decreasing plasma density at nighttime); the daytime increasing rate related to the refilling ranged from  $\sim 250$  to  $\sim 13$   $\text{amu}\cdot\text{cm}^{-3} \text{ h}^{-1}$  over  $L=2.3$ – $3.8$ , meaning upward plasma flux at the 1000km height in the range of  $0.9$ – $5.2\times 10^8$   $\text{amu}\cdot\text{cm}^{-2} \text{ s}^{-1}$ . They also determined the daily-averaged refilling rate to be  $\sim 420$   $\text{amu}\cdot\text{cm}^{-3} \text{ d}^{-1}$  at  $L=2.9$ – $3.1$ , including the nighttime downward flux. By comparison with Imager for Magnetopause-to-Aurora Global Exploration-EUV and VLF whistler data, they also estimated the plasma composition: The estimated  $\text{O}^+$  proportion was 3–7% at  $L=2.3$  and 6–13% at  $L=3.0$ .

For 19 cases during the interval over 50 days in May–July 2000 and 1 day in May 2008, Obana et al. (2010b) compared the plasmapause location determined by using extreme ultraviolet (EUV) images with that determined by using ground magnetometer data. In EUV images the plasmapause was identified as a sharp gradient in the brightness of the 30.4nm  $\text{He}^+$  emission; Obana et al. examined EUV images obtained by the IMAGE and the Kaguya satellites, operated in a solar maximum and minimum periods, respectively. With the ground magnetometer data, the plasmapause was identified as a sharp-drop point in the radial profile of the mass density, which was inferred from the field-line-resonance frequency (in the ULF ( $\sim 1$ – $1000$ Hz) band), identified in the ground-magnetometer data by applying to them the cross-phase method. The two kinds of the plasmapause measurements were compared in the same meridian at the same time, and very good agreement was found in 18 out of the 19 cases, suggesting that the  $\text{He}^+$ -plasmapause and the mass density-plasmapause are usually detected at the same place (with the error range of  $\pm 0.4R_E$ ). In only one case, the  $\text{He}^+$ -plasmapause and the mass density-plasmapause were not colocated; the difference was ascribed to the difference in the refilling time between  $\text{He}^+$  and other dominant species.

Nose (2010) examined if the bursty bulk flow (BBF) or the cavity mode resonance was more plausible as the excitation mechanisms for low-latitude Pi2 pulsations. He started from the following working assumption: In the case of the cavity mode resonance the wave period of Pi2 pulsations depends on the size and the plasma mass density of the plasmasphere, while in the case of the BBF-driven process the wave period is controlled by the BBF period and is independent of the plasmaspheric parameters. Then he investigated long-term (from March 1983 to October 2009) variation in Pi2 wave period observed at the

Kakioka observatory. Multiple correlation analysis revealed that the Pi2 period was negatively correlated with the  $\Sigma Kp$  index and positively correlated with ion mass in the near-Earth plasma sheet or the F10.7 index. Here the  $\Sigma Kp$  index was used as a proxy for the size of the plasmasphere, and the plasma sheet ion mass or the F10.7 index was used as a proxy for the mass density of the plasmasphere. The above-stated statistical result indicated that the Pi2 period was proportional to both the size and mass density of the plasmasphere, strongly supporting the plasmaspheric cavity mode resonance as the excitation mechanism of low-latitude Pi2 pulsations.

## References

- Ikeda, A., K. Yumoto, T. Uozumi, M. Shinohara, K. Nozaki, A. Yoshikawa, V. V. Bychkov, and B. M. Shevtsov (2010), Phase relation between Pi2-associated ionospheric Doppler velocity and magnetic pulsations observed at a midlatitude MAGDAS station, *J. Geophys. Res.*, 115, A02215, doi:10.1029/2009JA014397.
- Obana, Y., F. W. Menk, and I. Yoshikawa (2010a), Plasma refilling rates for  $L = 2.3$ – $3.8$  flux tubes, *J. Geophys. Res.*, 115, A03204, doi:10.1029/2009JA014191.
- Obana, Y., G. Murakami, I. Yoshikawa, I. R. Mann, P. J. Chi, and M. B. Moldwin (2010b), Conjunction study of plasmopause location using ground-based magnetometers, IMAGE-EUV, and Kaguya-TEX data, *J. Geophys. Res.*, 115, A06208, doi:10.1029/2009JA014704.
- Nose, M. (2010), Excitation mechanism of low-latitude Pi2 pulsations: Cavity mode resonance or BBF-driven process?, *J. Geophys. Res.*, 115, A07221, doi:10.1029/2009JA015205.
- Fujita, S., T. Tanaka, and T. Motoba, Long-period ULF waves driven by periodic solar wind disturbances, Symposium on Electromagnetospheric Physics, Recent Hotel, Fukuoka, Mar. 3–4, 2010.
- Kitamura, Kentarou, Satoko Saita, Shinichi Watari, Hisao Yamagishi, and Takahiro Obara, Relationships between High-latitude Pc5 and MeV electron flux at the geosynchronous orbit, Japan Geoscience Union Meeting 2010, May 23–28 2010 at Makuhari, Chiba, Japan.
- Fujimoto, Akiko, Shuji Abe, and Kiyohumi Yumoto, Estimation of the radial diffusion coefficient using REE-associated ground Pc 5 pulsations, Japan Geoscience Union Meeting 2010, May 23–28 2010 at Makuhari, Chiba, Japan.
- Ikeda, Akihiro, Kiyohumi Yumoto, Manabu Shinohara, Kenro Nozaki, Akimasa Yoshikawa, Toshiki Shimbaru, Akiko Fujimoto, B. M. Shevtsov, V. V. Bychkov, Q. M. Sugon, Jr., and D. McNamara, Ionospheric Electric and Ground Magnetic Pc 5 Variations at Lowlatitude and Equatorial MAGDAS Stations, Japan Geoscience Union Meeting 2010, May 23–28 2010 at Makuhari, Chiba, Japan.
- Saka, Osuke, and Kanji Hayashi, Pi2 modulation of aurora activities and ground-satellite magnetometer data by a periodic passage of plasma flows, Japan Geoscience Union Meeting 2010, May 23–28 2010 at Makuhari, Chiba, Japan.
- Obana, Yuki, Ichiro Yoshikawa, Frederick W. Menk, Colin L. Waters, Murray D. Sciffer, Akimasa Yoshikawa, Mark Moldwin, Ian R. Mann, and David Boteler, Latitudinal distribution of quarter-wave length, standing Alfvén modes, Japan Geoscience Union Meeting 2010, May 23–28 2010 at Makuhari, Chiba, Japan.
- Yoshikawa, Akimasa, Olaf Amm, and Ryoichi Fujii, Formation of Cowling channel through the ionosphere-magnetosphere coupling via shear Alfvén wave, Japan Geoscience Union Meeting 2010, May 23–28 2010 at Makuhari, Chiba, Japan.
- Nomura, Reiko, Kazuo Shiokawa, Kaori Sakaguchi, Yuichi Otsuka, and Martin Connors, Polarization of Pc1/EMIC waves and related aurora observed at Athabasca, Japan Geoscience Union Meeting 2010, May 23–28 2010 at Makuhari, Chiba, Japan.
- Nose, Masahito, Excitation mechanism of low-latitude Pi2 pulsations: Cavity mode resonance or BBF-driven process?, Japan Geoscience Union Meeting 2010, May 23–28 2010 at Makuhari, Chiba, Japan.

- Sakai, Mina, Naoko Horikawa, Teiji Uozumi, Shuji Abe, and Kiyohumi Yumoto, Characteristics of Dayside Pi 2 Pulsations Observed MAGDAS/CPMN Stations, Japan Geoscience Union Meeting 2010, May 23-28 2010 at Makuhari, Chiba, Japan.
- Pilipenko, Viacheslav, A. Schekotov, and Kazuo Shiokawa, ULF magnetic response to lightning, Japan Geoscience Union Meeting 2010, May 23-28 2010 at Makuhari, Chiba, Japan.
- Sakurai, Tohru, Reexamination on Pi 1/2 pulsation onsets as a substorm onset indicator, Japan Geoscience Union Meeting 2010, May 23-28 2010 at Makuhari, Chiba, Japan.
- Saka, Osuke, and Kanji Hayashi, The first 10-min interval of Pi2 onset during expansion of energetic ion regions from dusk to dawn sector, Japan Geoscience Union Meeting 2010, May 23-28 2010 at Makuhari, Chiba, Japan.
- Nariyuki, Yasuhiro, Tohru Hada, and Ken Tsubouchi, Heating and acceleration of ions in non-resonant solar wind Alfvénic turbulence, Japan Geoscience Union Meeting 2010, May 23-28 2010 at Makuhari, Chiba, Japan.
- Iyemori, Toshihiko, Kent Taira, and Mitsuru Matsumura, Ionospheric currents and micropulsations caused by the lower atmospheric disturbances, Japan Geoscience Union Meeting 2010, May 23-28 2010 at Makuhari, Chiba, Japan.
- Koshida, Tomonori, Takashi F. Shibata, Satoshi Taguchi, and Hiroaki Misawa, Characteristics of Jovian ionospheric Alfvén resonator observed by using wave modulations of L-burst emissions, Japan Geoscience Union Meeting 2010, May 23-28 2010 at Makuhari, Chiba, Japan.
- Febriani, Febty, Takuya Hirano, Katsumi Hattori, and Kazuo Shiokawa, ULF Electromagnetic Anomaly Associated with Two Large 2009 Earthquakes in Indonesia, Japan Geoscience Union Meeting 2010, May 23-28 2010 at Makuhari, Chiba, Japan.
- Kawano, Hideaki, Satoko Saita, Genta Ueno, Tomoyuki Higuchi, Shin'ya Nakano, and Kiyohumi Yumoto, Toward estimating the plasmaspheric plasma density by combining ground-magnetometer data and GPS-TEC data, Japan Geoscience Union Meeting 2010, May 23-28 2010 at Makuhari, Chiba, Japan.

### **Pc1 wave observations by ground magnetometer**

Solar-Terrestrial Environment Laboratory, Nagoya University continues routine operation of five induction magnetometers at Far-Eastern Russia, Japan, and Canada. The quick-look data are available at <http://stdb2.stelab.nagoya-u.ac.jp/magne/index.html>. Investigations are under way for polarization characteristics of Pc1 pulsations and harmonic structures in the ionospheric Alfvén resonator.

### **Computer Simulation**

Development of numerical scheme for Vlasov code: A robust numerical interpolation scheme for Vlasov code simulations is developed by using a positive, non-oscillatory and conservative limiter [Umeda, 2008]. The new Vlasov code is applied for parametric decay of Langmuir wave packets in space plasmas. It is shown that Langmuir waves decay into back-scattered Langmuir waves and ion acoustic waves when the wave power of parent Langmuir waves is larger than the thermal energy of background plasmas [Umeda and Ito, 2008]. A new two-dimensional Vlasov code including fully electromagnetic fields is also developed. The two-dimensional Vlasov code is successfully applied to the GEM magnetic reconnection challenge problem [Umeda et al., 2009]. The conservative limiter is also extended for application to MHD simulations [Tanaka et al., 2009].

Simulation of shock : A new two-dimensional shock-rest-frame model for full particle simulations is developed by Umeda et al. [2008]. The new model allows us to follow full-kinetic dynamics of collisionless shocks in a long-time simulation run. It is shown that shock front ripples enhance nonthermal electrons, suggesting that ion dynamics plays important roles in electron acceleration [Umeda et al. 2009].

Simulation of beam-plasma interactions: Generations of electromagnetic wave modes during electron beam-plasma interactions are studied by means of large-scale two-dimensional full particle simulations. When the relative bulk velocity between total electrons and background ions is faster than the Alfvén velocity, electromagnetic ion cyclotron waves are excited [Umeda, 2008]. When there are two counter-directional Langmuir waves, electromagnetic light mode waves are excited by a three-wave interaction [Umeda, 2010]. It is also shown that induced back-scattering of Langmuir waves by thermal ions is stronger than the back-scattering of Langmuir waves by parametric decay.

PIC simulation of whistler turbulence: Whistler turbulence cascade is studied to understand essential properties of the energy spectrum at electron scales, by using a two-dimensional electromagnetic particle-in-cell (PIC) simulation. The simulation shows that the magnetic energy spectrum of forward-cascaded whistler turbulence exhibits a steeper power-law spectrum around an electron inertial scale than that predicted by EMHD simulations and theories. A comparison of the spectral index from the PIC simulation with that predicted by the scaling law for short scales, suggests that the energy cascade at short scales includes the effect of not only magnetic fluctuations but also electron velocity fluctuations. The steep magnetic spectrum may support recent solar wind observations at the electron scales.

MHD simulation for Kelvin-Helmholtz instability: 2D-MHD simulation of the Kelvin-Helmholtz instability in a large simulation domain shows rapid formation of a broad plasma turbulent layer is possible by forward and inverse energy cascade processes. The forward energy cascade is triggered by the secondary Rayleigh-Taylor instability [Matsumoto and Hoshino, GRL, 2004] and the inverse cascade is accomplished by nonlinear mode couplings between the fastest growing mode and other KH unstable modes. The results resemble observational characteristics of the low-latitude boundary layer of the magnetosphere.

#### **References:**

- Matsumoto, Y., and K. Seki, Formation of a broad plasma turbulent layer by forward and inverse energy cascades of the Kelvin-Helmholtz instability, *J. Geophys. Res.*, doi:10.1029/2009JA014637, in press.
- Umeda, T., A conservative and non-oscillatory scheme for Vlasov code simulations, *Earth, Planets and Space*, Vol.60, No.7, pp.773-779, 2008.
- Umeda, T., and T. Ito, Vlasov simulation of Langmuir decay instability, *Physics of Plasmas*, Vol.15, No.8, 084503 (4pp.), 2008.
- Umeda, T., K. Togano, and T. Ogino, Two-dimensional full-electromagnetic Vlasov code with conservative scheme and its application to magnetic reconnection, *Computer Physics Communications*, Vol.180, No.3, pp.365-374, 2009.
- Tanaka, S., T. Umeda, Y. Matsumoto, T. Miyoshi, and T. Ogino, Implementation of non-oscillatory and conservative scheme into magnetohydrodynamic equations, *Earth, Planets and Space*, Vol.61, No.7, pp.895-903, 2009.
- Umeda, T., M. Yamao, and R. Yamazaki, Two-dimensional full particle simulation of a perpendicular collisionless shock with a shock-rest-frame model, *Astrophysical Journal Letters*, Vol.681, No.2, pp.L85-L88, 2008.
- Umeda, T., M. Yamao, and R. Yamazaki, Electron acceleration at a low-Mach-number perpendicular collisionless shock, *Astrophysical Journal*, Vol.695, No.1, pp.574-579, 2009.
- Umeda, T., Generation of low-frequency electrostatic and electromagnetic waves as nonlinear consequences of beam-plasma interactions, *Physics of Plasmas*, Vol.15, No.6, 064502 (4pp.), 2008.
- Umeda, T., Electromagnetic plasma emission during beam-plasma interaction: Parametric decay versus induced scattering, *Journal of Geophysical Research*, Vol.115, No.A1, A01204 (6pp.), 2010.

#### **Lightning-generated sferics observations**

To extract information on return stroke from sferics, Ozaki et al. [2010a, b] have been

investigating a technique for estimating return stroke current. They have succeeded in obtaining information on discharge time of the return stroke from the spheric spectrum, which is given by a sinc function of discharge time. They reconstructed the return stroke current waveforms by using the least-square method with the estimate value of the discharge time. By the numerical simulation, they confirmed that the error in the estimation of the current moment is less than 10% for the horizontal distances over 100 km from the lightning.

#### References:

Ozaki, M., S. Yagitani, T. Koide, and I. Nagano, "Estimation of lightning return stroke current waveforms by nonlinear least squares method applied to spherics," IEICE Transactions on Communications, Vol.J93-B, No.4, pp.711-720, April, 2010a.

Ozaki, M., S. Yagitani, T. Koide, Y. Itoh, and I. Nagano, "Extracting return stroke current moment based on spheric spectrum," Proc. AP-RASC'10, Toyama, Japan, September, 2010b.

#### Conferences and Meetings

- 1) 2010 Western Pacific Geophysics Meeting 22-25 June 2010, Taipei, Taiwan  
Meeting web site: <http://www.agu.org/meetings/wp10/>
- 2) Second International Symposium on Radio Systems and Space Plasma, August 25-27, 2010, Sofia, Bulgaria
- 3) AP-RASC'10, Toyama, Japan, 22-26 September 2010, Toyama, Japan  
The following papers will be presented in AP-RASC'10.

Fukuhara H. et al., DEVELOPMENT OF MINIATURIZED OBSERVATION SYSTEM FOR PLASMA WAVE USING ANALOG ASIC FOR SMALL SCIENTIFIC SATELLITE MISSIONS, HBCGb-1.

Goto Y. et al., MODELING OF THE PLASMASPHERIC DENSITY PROFILE FROM LARGE DATA SETS OF VLF WAVES AND GPS SIGNALS, HFG-4(Invited).

Hashimoto K. et al., ELECTROSTATIC SOLITARY WAVES NEAR THE MOON OBSERVED BY KAGUYA, HG2b-6.

Hayashi S. et al., EXAMINATION OF VALIDITY OF THE GLOBAL CORE PLASMA MODEL USING WHISTLER DISPERSIONS OBTAINED BY THE AKEBONO, HP-9.

Higashi R. et al., STATISTICAL ANALYSIS OF ANTENNA IMPEDANCE ONBOARD AKEBONO SATELLITE, HP-6.

Higuchi T. and R.Yoshida, EASY AND SIMPLE PARAMETER ESTIMATION METHODS IN THE SIMULATION MODEL FOR DATA ASSIMILATION, HFG-6(Invited).

Hikishima M. et al., MICROBURST PRECIPITATION OF ENERGETIC ELECTRONS ASSOCIATED WITH CHORUS WAVE GENERATION, HG2a-4.

Hirono T. et al., PARTICLE SIMULATIONS ABOUT GENERATION MECHANISM OF LOW FREQUENCY COMPONENT OF BEN, HP-15.

Imachi T. et al., CHARACTERISTICS OF WIRE ANTENNA FOR PLASMA WAVE OBSERVATION AT LOW FREQUENCIES, HBCGa-3.

Ishisaka K. et al., INVESTIGATION OF CHARACTERISTICS OF RADIO WAVES PROPAGATIONS IN THE LOWEST IONOSPHERE BY S-310-40 SOUNDING ROCKET MEASUREMENT, HBCGa-6.

Ishisaka K. et al., INVESTIGATION OF RELATIONSHIP BETWEEN SPACECRAFT POTENTIAL AND ELECTRON DENSITY BY AKEBONO SATELLITE, HP-5.

Iwai K. et al., A WIDE BAND SPECTRO-POLARIMETER FOR GROUND-BASED METRIC SOLAR RADIO BURSTS OBSERVATION OF TOHOKU UNIVERSITY, HBCGb-6.

Jin H. et al., THE FIRST FULLY-COUPLED WHOLE ATMOSPHERE-IONOSPHERE SIMULATION MODEL: INITIAL RESULTS AND FUTURE DIRECTION, HFG-1.

Kasahara Y. et al., LUNAR WAKE STRUCTURE AND ITS ELECTRON DENSITY PROFILE IN THE SOLAR WIND OBSERVED BY KAGUYA LRS/WFC, HG2c-6.

Katoh Y. and Y. Omura, ELECTRON HYBRID SIMULATION OF NONLINEAR GROWTH OF WHISTLER-MODE WAVES IN THE EQUATORIAL REGION OF THE INNER MAGNETOSPHERE, HG1a-2(Invited).

Katoh Y. and Y. Omura, CROSS-ENERGY COUPLING IN THE PROCESS OF WHISTLER-MODE WAVE-PARTICLE INTERACTIONS IN THE EARTH'S INNER MAGNETOSPHERE, HG2a-6.

Kidani Y. et al., ON THE REFORMATION AT PERPENDICULAR SHOCKS, HP-14.

Kitaguchi S. et al., PLASMA WAVES OVER LUNAR MAGNETIC ANOMALIES OBSERVED BY LRS/WFC ONBOARD KAGUYA, HP-16.

Kondo T. et al., A SAMPLER UNIT PLANNED TO THE LLFAST (LUNAR LOW FREQUENCY ASTRONOMY TELESCOPE) PROJECT DEDICATED TO MOON-EARTH VLBI OBSERVATIONS, HBCGb-5.

Kumamoto A. et al., DEVELOPMENT OF RADAR SOUNDER AND IMPEDANCE PROBE FOR OBSERVATIONS IN THE FUTURE PLANETARY MISSIONS, HBCGa-2(Invited).

Matsuda K. et al., SIMULATION STUDY ON ASYMMETRICAL FEATURES OF FREQUENCY AND INTENSITY IN THE IO-RELATED DECA-METRIC RADIO SOURCES, HP-13.

Matsukiyo S. and M.Scholer, KINETICS OF HIGH ENERGY ELECTRONS IN NONSTATIONARY QUASIPERPENDICULAR SHOCKS, HG2c-5.

Miyake Y. et al., PARTICLE-IN-CELL ANALYSIS OF A SPACE-BASED ELECTRIC FIELD INSTRUMENT SURROUNDED BY A PHOTOELECTRON CLOUD, HBCGa-4.

Miyashita Y. et al., NONLINEAR EVOLUTION OF WHISTLER-MODE CHORUS WAVES, HP-18.

Miyoshi Y. and R. Kataoka, FLUX ENHANCEMENT OF THE OUTER RADIATION BELT BY WHISTLER WAVES, HG2a-1(Invited).

Miyoshi Y. et al., DATA ASSIMILATION OF RELATIVISTIC ELECTRONS OF THE RADIATION BELTS, HP-11.

Mori S. et al., FREQUENCY AND AMPLITUDE VARIATION OF CHORUS EMISSIONS OBSERVED BY GEOTAIL, HP-17.

Moritaka T. et al., SOLAR WIND INTERACTION WITH A SMALL SCALE ARTIFICIAL MAGNETOSPHERE FOR MAGNETO-PLASMA SAIL, HG1b-2.

Murase Y. et al., DEVELOPMENT OF A HIGH-ACCURACY RADIO CLOCK RECEPTION SYSTEM, HP-4.

Murata K. T. et al., A SCIENCE CLOUD AT NICT FOR SPACE WEATHER RESEARCHES, HG1b-4.

Nakajo T. et al., 500 KM-CLASS DUAL FREQUENCY VLBI OBSERVATION OF JOVIAN DECA-METER RADIATION, HBCGb-4.

Nakamura, M. S., A 3D HYBRID CODE FOR MINI-MAGNETOSPHERE SIMULATION, HG1b-3.

Nakamura T. K., DISPERSION SOLVER BY RATIONAL FUNCTIONS, HG1a-5.

Nakano S. et al., AN EUV DATA ASSIMILATION TECHNIQUE FOR THE MODELING OF THE PLASMASPHERE USING THE PARTICLE FILTER, HP-10.

Nariyuki Y. et al., HEATING AND ACCELERATION OF SOLAR WIND IONS IN NON-RESONANT ALFVENIC TURBULENCE, HG1b-1.

Nishiyama T. et al., FINE SCALE PRECIPITATIONS OF AURORAL ELECTRONS DUE TO THE RESONANT INTERACTION WITH WHISTLER MODE WAVES, HG2a-5.

Oike Y. et al., EVALUATION OF DATA SELECTION ALGORITHM IMPLEMENTED IN THE LRS/WFC ONBOARD KAGUYA, HP-2.

Okada S. et al., STUDY ON THE SMALL SENSOR NODE SYSTEM FOR MEASURING SPACE ELECTROMAGNETIC ENVIRONMENT, HP-1.

Omura Y. et al., THEORY AND OBSERVATION OF ELECTROMAGNETIC ION CYCLOTRON TRIGGERED EMISSIONS IN THE MAGNETOSPHERE, HG2b-1(Invited).

Saito A. et al., IONOSPHERIC TOMOGRAPHY WITH CONSTRAINED LEAST-SQUARES METHOD USING GPS TOTAL ELECTRON CONTENT DATA, HP-8.

Saito S. et al., WHISTLER TURBULENCE IN ELECTRON SCALES: PARTICLE-IN-CELL SIMULATIONS, HG2c-4.

Sato Y. et al., AKEBONO SATELLITE OBSERVATIONS OF MF/HF AURORAL RADIO EMISSIONS EMANATING FROM THE TOPSIDE IONOSPHERE, HG2c-2.

Seko H. et al., GPS METEOROLOGY: ATMOSPHERIC STUDIES USING RADIO WAVES FROM GPS SATELLITES, HFG-2(Invited).

Shiraishi T. et al., ANALYSIS OF LOW-FREQUENCY PLASMA WAVE OBSERVED BY WAVEFORM CAPTURE (WFC) ONBOARD KAGUYA, HP-21.

Shoji M. and Y.Omura, ELECTROMAGNETIC ION CYCLOTRON TRIGGERED EMISSIONS IN A DIPOLE GEOMETRY: HYBRID SIMULATION RESULTS, HG2b-2.

Sugiyama H. et al., DATA ANALYSIS OF NON-THERMAL PLASMA PARTICLES OBSERVED BY KAGUYA SPACECRAFT ORBITING AROUND THE MOON, HP-22.

Takahashi K. et al., STATISTICAL ANALYSIS OF LH PLASMA WAVES OBSERVED BY GEOTAIL SPACECRAFT, HP-20.

Takenaka S. et al., DEVELOPMENT OF A CO-OPERATIONAL OBSERVATION SIMULATOR FOR FORMATION-FLYING MAGNETOSPHERIC EXPLORATION MISSION, HBCGa-5.

Tokumaru M. et al., A NEW RADIOTELESCOPE FOR INTERPLANETARY SCINTILLATION OBSERVATIONS; SOLAR WIND IMAGING FACILITY, HBCGb-2(Invited).

Tomita S. et al., THE DEVELOPMENT OF A RADIO WAVE RECEIVER FOR NEXT MARS LANDER DEPLOYMENT, HP-3.

Umeda T., ELECTROMAGNETIC PLASMA EMISSION DURING BEAM-PLASMA INTERACTION, HG1a-4(Invited).

Yoshikawa M. et al., EVOLUTION OF ENERGETIC ELECTRON DISTRIBUTION DUE TO INTERACTION WITH CHORUS EMISSIONS, HP-19.

### **Acknowledgement:**

The editors thank Dr. Y. Kasahara, Dr. S.Yagitani, Dr. A. Kumamoto, Dr. H. Kawano and Dr. Y. Miyoshi for their contribution to this report.